Reactive and Functional Polymers 168 (2021) 105058

Contents lists available at ScienceDirect

Reactive and Functional Polymers

journal homepage: www.elsevier.com/locate/react

Perspective Article

N-halamine-decorated electrospun polyacrylonitrile nanofibrous membranes: characterization and antimicrobial properties

Martha Y. Garcia Cervantes [a], Li Han [b], Jean Kim [b], Basant Chitara [a], Nathan Wymer [a], Fei Yan [a,*]

[a] Department of Chemistry and Biochemistry, North Carolina Central University, Durham, NC 27707, USA
[b] RTI International, Research Triangle Park, NC 27709, USA

ARTICLE INFO

Keywords:
Electrospinning
N-Halamines
Antimicrobial
Bioaerosol
Composite Nanofibers

ABSTRACT

Microbial contamination of drinking water and air is an alarming phenomenon that has attracted increasing global attention. Although many advances in microbial disinfection have been made over the years, robust, rapid, inexpensive and field-deployable strategies are still urgently needed to address this public health issue. Herein we report the preparation of antimicrobial nanofibrous membranes, which involves incorporation of highly porous electrospun polyacrylonitrile (PAN) membranes with 1-chloro-2,2,5,5-tetramethyl-4-imidazolidinone (MC) by two different approaches, namely, blend electrospinning and soaking. The functionalized membranes were characterized using scanning electron microscopy, Fourier transform infrared spectroscopy, and titrimetry, and their antimicrobial efficacies were evaluated against two bacteria (*Klebsiella pneumoniae* and *Escherichia coli*). The MC-decorated electrospun PAN membranes inactivated both bacterial strains within 2 min of contact time. Moreover, the MC-soaked PAN membrane showed excellent disinfection efficacy against aerosolized *E. coli* after an exposure of 30 min. The simplicity, cost-effectiveness, versatility, and scalability of the electrospinning process, together with the superior antimicrobial activity of N-halamines make it a promising solution for water disinfection, and for the inactivation of airborne microorganisms.

1. Introduction

Pathogens, including viruses and bacteria in water and air, represent serious health concerns around the globe [1,2]. Contaminated water and poor sanitation are linked to transmission of waterborne diseases such as cholera, diarrhoea, dysentery, hepatitis A, typhoid, and polio. According to a report by the World Health Organization (WHO), approximately 800,000 people are estimated to die each year from diarrhoea alone, however, the deaths of ~300,000 children under the age of 5 could be avoided each year if appropriate drinking-water quality guidelines could be implemented [3]. Caused by severe acute respiratory syndrome coronavirus 2 (SARS-CoV-2), COVID-19 became the most well-known airborne disease since 2020. To date, SARS-CoV-2 has infected about 172 million cases worldwide and resulted in at least 3.7 M deaths [4]. Other types of airborne diseases include the flu, tuberculosis, chickenpox, measles, mumps, and whooping cough. Many advances in microbial disinfection have been made over the years including filtration [5], photosensitization [6], UV radiation [7], and photocatalysis [8], to name just a few. However, there is an increasing need for robust, rapid, inexpensive and field-deployable strategies to address this public health issue. Among which, antimicrobial electrospun materials emerge as one of the most promising solutions to this problem [9].

Electrospinning is a very versatile technique that has been used in many applications, such as tissue engineering [10], textiles [11], air and water treatment filter [12,13], solar cells [14,15], drug delivery systems [16,17], and chemical sensing [18,19], among others. During the past two decades, electrospinning has evolved from a single-fluid blending process [20] to coaxial [21], tri-axial [22], side-by-side [23,24], and other complicated multiple-fluid processes [25]. These processes are useful for improving the encapsulation efficiency. However, the traditional method, soaking, comprises a widely adopted method for loading active ingredients onto pre-made electrospun polymeric substrates. In the present work, the preparation of N-halamine-functionalized electrospun PAN nanofibers was carried out using two different methods. i.e. blend electrospinning and soaking, and the resulting nanocomposites were evaluated for their antibacterial efficacies against two bacteria (*Klebsiella pneumoniae* and *Escherichia coli*). Blend electrospinning involves the mixing of an N-halamine compound with the PAN polymeric solution prior to electrospinning process, and soaking is performed by putting the electrospun PAN nanofibers in an N-halamine ethanolic

* Corresponding author.
E-mail addresses: lhan@rti.org (L. Han), jeankim@rti.org (J. Kim), fyan@nccu.edu (F. Yan).

https://doi.org/10.1016/j.reactfunctpolym.2021.105058
Received 8 June 2021; Received in revised form 25 September 2021; Accepted 28 September 2021
Available online 30 September 2021

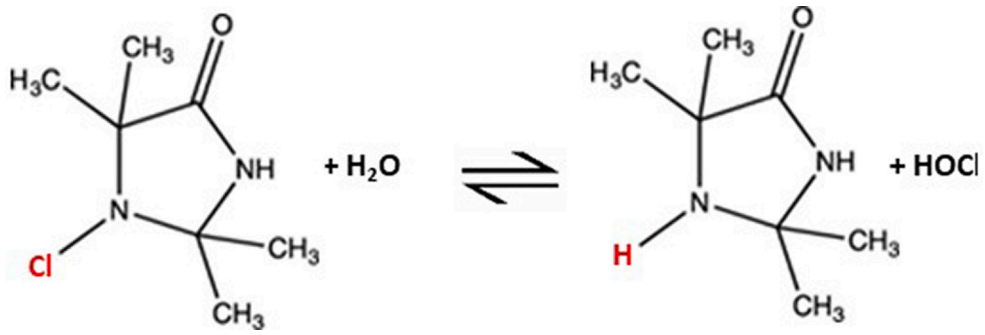

Fig. 1. The hydrolysis of MC produces hypochlorous acid (HOCl), which leads to inactivation of microorganism.

solution for 2 min.

Because of their unique properties including high surface area, large porosity, and lightweight, functionalized electrospun nanofibers with antimicrobial activity have attracted increasing attention in a variety of applications such as tissue engineering [26], drug delivery [27], filtration [28], protective clothing [29], wound dressing [30], and sensor devices [31]. Several antimicrobial agents such as metal (e.g. Ag, Cu, Zn) nanoparticles [32], metal oxide (e.g., ZnO) nanoparticles [33], phosphonium salts [34], quaternary ammonium compounds [35], and N-halamines [36] have been used to introduce additional antimicrobial functions into electrospun fibers. Among these, N-halamines are one of the most effective disinfectant agents [37]. N-halamines are compounds in which one or more oxidative halogens (X = Cl, Br, I) are covalently bonded to nitrogen. Because of the strong oxidative state (+1) of halogen atoms in these N − X covalent bonds, N-halamines have demonstrated excellent antimicrobial activities against a wide range of microorganisms such as fungi [38], bacteria [39], yeasts [40], and viruses [41], without causing the microorganisms to develop resistance to them [42]. During the inactivation of microorganisms, the N-X bond is converted to N—H bond, which results in a reduction of antimicrobial activity of N-halamines [43]. The activity, however, can be easily recovered through exposure to dilute household bleach or halogen-releasing agents [44].

In this work, N-halamine-decorated electrospun PAN nanofibrous membranes were fabricated for disinfecting liquid bacterial suspensions and bacterial bioaerosols. 1-chloro-2, 2, 5, 5-tetramethyl-4-imidazolidinone (MC, see Fig. 1) was selected as a model N-halamine. MC is also the active ingredient in Tetra™ LifeGuard tablets that have been used for treating most common fish diseases [45]. PAN is a hydrophobic polymer with excellent chemical and thermal characteristics [46]. It has been widely used in textiles, ultra-filtration membranes, and reverse osmosis because of its excellent permeability, high biostability and resistance to degradation [47]. MC-decorated PAN membranes, i.e., 0.5 wt%-soaked PAN and 1.0 wt% MC-embedded PAN were prepared via a simple post-treatment process, and a one-step electrospinning process, respectively. Subsequently, the oxidative chlorine content in MC-decorated PAN membranes was determined by iodometric/thiosulfate titration, and their surface functional groups and morphology were examined by attenuated total reflection Fourier transform infrared (ATR-FTIR) spectroscopy and scanning electron microscopy (SEM), respectively. Finally, the antimicrobial efficacies of MC-decorated PAN membranes were evaluated against strains of *K. pneumoniae* subsp. *pneumoniae* (ATCC 13882) and *E. coli* (K12 and ATCC 15997 as an aerosol challenge).

2. Experimental

2.1. Materials

Polyacrylonitrile (PAN), with a molecular weight of 150,000 Da was purchased from Sigma Aldrich (St. Louis, MO). *N*, *N*-dimethylformamide (DMF), 99.9% and sodium thiosulfate were purchased from Acros Organics (ThermoFisher; Waltham, MA). 1-chloro-2, 2, 5, 5-tetramethyl-4-imidazolidinone (MC), was obtained from RTI International (Research Triangle Park, NC). *Klebsiella pneumoniae* (*K. pneumoniae*, Gram-negative bacteria, ATCC 13882) and *Escherichia coli* (*E. coli*, Gram-negative bacteria, K12 ((10G; Lucigen) and ATCC 15597) were purchased from the American Type Culture Collection (ATCC; Manassas, VA). The power supply was from Gamma High Voltage Research (ES40P-20 W/DA), the syringe pump was from KD Scientific (KDS-100), and the dehumidifier from Comfort-Aire (BHD-301-H). All microbial samples were handled and disposed of using appropriate biosafety guidelines.

2.2. Electrospinning of PAN membranes

The spinning solution was prepared by adding 1.3 g PAN into 15 mL DMF followed by mechanical stirring at 1000 rpm overnight at ambient temperature until a homogeneous solution was achieved. The solution was then transferred into a 10 mL plastic syringe equipped with a 21-gauge blunt probe needle. When the electrospinning process was performed, a DC voltage of 15 kV was applied, the tip to collector distance was set as 13 cm, and the flow rate of the syringe pump was set at 2.5 mL/h. The collector was a round 20-cm aluminum plate covered with aluminum foil. Electrospinning was allowed to continue until all 10 mL of solution were dispensed. The resulting membrane was carefully peeled from the collection plate for further analysis and subsequent treatment.

2.3. Incorporation of MC into electrospun PAN membranes

2.3.1. Preparation of 1.0 wt% MC-embedded PAN membranes

This electrospinning process was carried out according to a previously reported procedure [48] with slight modifications. Specifically, the spinning solution was prepared by first adding 1.3 g PAN into 15 mL DMF followed by mechanical stirring at 1000 rpm overnight at ambient temperature until all PAN polymers were fully dissolved. Subsequently, 0.156 g MC or 1.0 wt% MC was dissolved in the homogeneous PAN solution by stirring for 2 h. The mixture was then transferred into a 10 mL plastic syringe equipped with a 21-gauge blunt probe needle. The 1.0 wt% MC-embedded PAN membranes were prepared by applying a DC voltage of 13 kV with a syringe pump setting of 1.5 mL/h.

2.3.2. Preparation of 0.5% wt MC-soaked PAN membranes

0.039 g MC was dissolved into 10 mL ethanol at room temperature to make a 0.5 wt% MC solution. The as-prepared PAN membrane described earlier was cut into 2 cm × 2 cm coupons. Each coupon was soaked in the 0.5 wt% MC solution for 1 min then flipped and allowed to soak for another minute. The coupons were allowed to dry overnight at room temperature for further analysis and subsequent experiments.

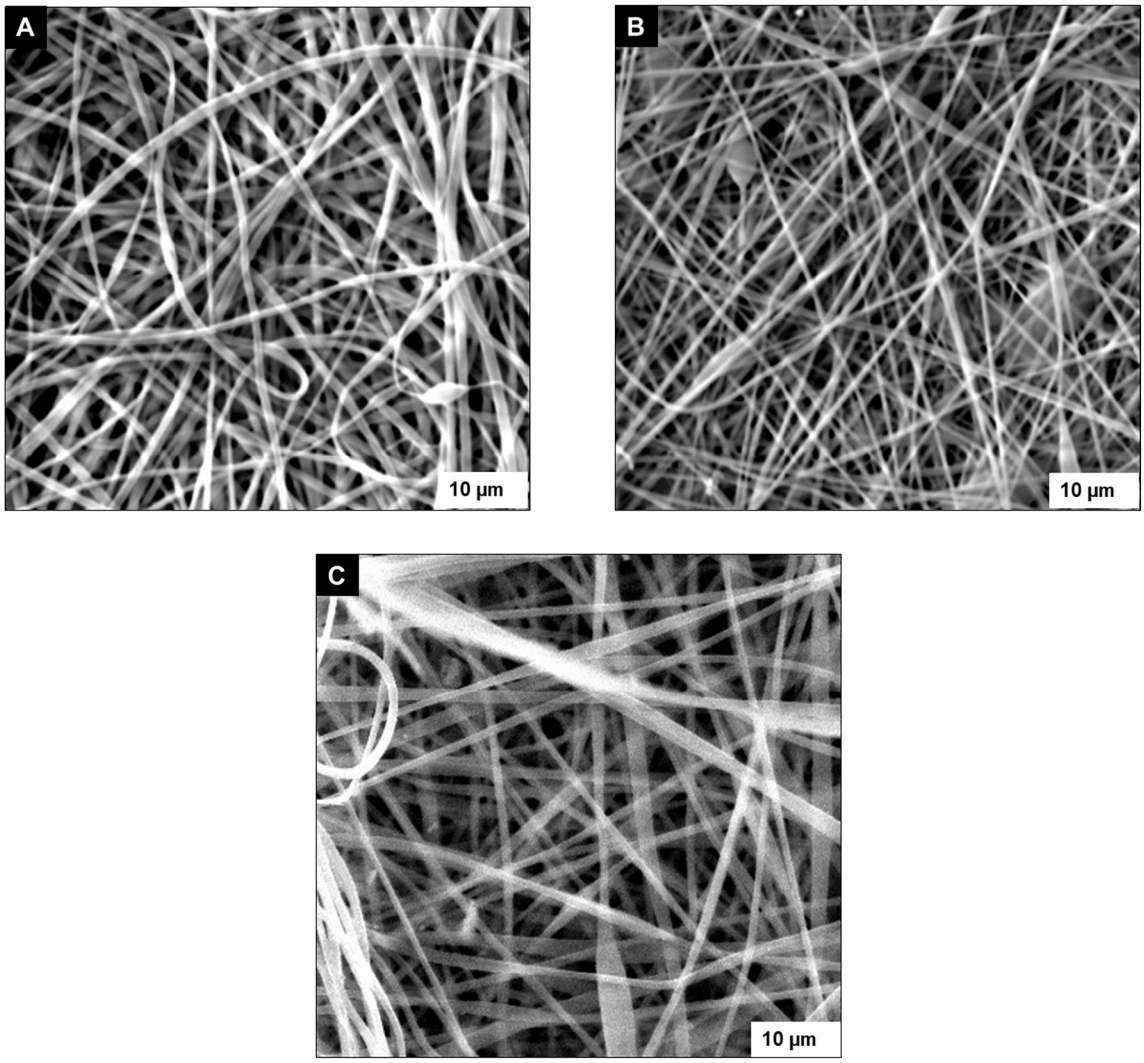

Fig. 2. SEM images of A) blank PAN nanofibers, (B) 0.5 wt% MC –soaked PAN nanofibers, and C) 1.0 wt% MC-embedded PAN nanofibers. Scale bar: 10 μm.

2.4. Assessment of oxidative chlorine content in MC-decorated PAN membranes

The oxidative chlorine content in MC-decorated PAN membranes was measured via a modified iodometric/thiosulfate titration procedure [49]. The weight percentage of oxidative chlorine content (Cl^+%) for the samples was calculated using the following equation:

$$Cl^+\% = \frac{35.45 \times M \times V \times 0.001}{W} \times 100$$

where M is the molarity (mol/L) of sodium thiosulfate (which is 0.5 mM in this current study). V is the volume (mL) of sodium thiosulfate consumed in the titration, and W is the weight (g) of the membrane.

2.5. Antimicrobial efficacy testing

2.5.1. Liquid bacterial suspensions

The AATCC Test Method 100–2004, "sandwich test" was used to determine the antimicrobial efficacy of the PAN nanofiber coupons before and after the incorporation of MC. *K. pneumoniae* (ATCC 13882) and *E. coli* (K12) were grown overnight in 20 mL Luria-Bertani (LB) broth in a 125 mL baffled flask at 37 °C/225RPM. The bacterial cells were washed three times with a sterile glycerol (20% v/v) and diluted using sterile 100 μM phosphate buffer (pH 7.4) to the desired colony-forming units (CFU). The overnight culture was measured at Abs_{600nm} with a Abs600nm = 1.0 equal 10^9 CFU/mL [50]. An aliquot of 50 μL of 10^6 CFU /mL suspension was added to the center of the first coupon, and a second coupon was placed on top. A sterile weight was placed on the second coupon to ensure good contact with the microorganisms. After a predetermined contact time, the first coupon was treated with 5 mL of 0.01 M sodium thiosulfate solution to neutralize chlorine residuals and terminate further disinfection. Samples were vigorously vortexed for 10 min to detach viable bacteria from the surface of the coupon. The extracts were 10-fold serially diluted using 100 μM phosphate buffer (pH 7.4), plated onto LB agar plates, and incubated at 37 °C for 24 h for viable counts. Each sample was run in triplicate, and the average value with 1 standard deviation (SD) was reported. All results were presented as means ± SD.

2.5.2. Bioaerosols

Three membrane types (Control PAN, 0.5 wt% MC-soaked PAN, and 1.0 wt% MC-embedded PAN) were loaded with aerosolized *E. coli* (ATCC 15597). The loading process was conducted using a collision nebulizer (BGI; Waltham, MA) and a mask testing chamber similar to the one described in the ASTM F2101 Test Method [51]. The collision was prepared using an overnight culture of *E. coli* in trypticase soy broth (TSB) diluted with buffered peptone water (BPW) at a final concentration of ~10^5 CFU/mL. Filtered air was applied to the collision at 12 psi

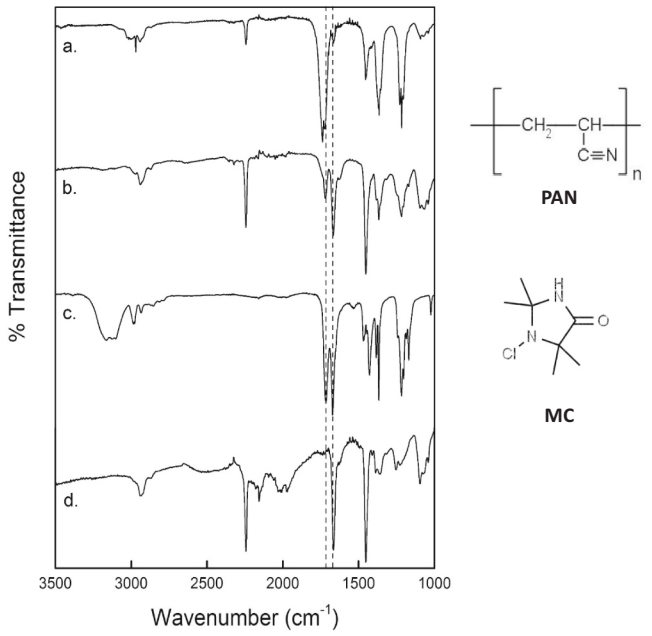

Fig. 3. FT-IR spectra of a) 0.5 wt% MC-soaked PAN nanofibers, b) 1.0 wt %-embedded PAN nanofibers, c) MC, and d) electrospun PAN nanofibers. Molecular formula of PAN and MC.

to generate an aerosol which was pulled through the chamber through a single stage impactor at 60 cubic feet per hour (CFH). The bioaerosol was loaded onto each membrane for 10 min and the loaded membranes were further incubated for 30 min at room temperature. *E. coli* was extracted from the membranes using 10 mL of 0.01 M sodium thiosulfate and shaken on a wrist action shaker (Burrell Scientific; Pittsburg, PA) for 15 min. The extracts were 10-fold serially diluted and plated onto TSA plates for viable counts. The aerosol loading for each membrane was done in triplicate and a mean CFU of viable bacteria was determined.

2.6. Characterization of physicochemical properties

Scanning electron microscopy (SEM) images were examined by an FEI Quanta 200 Environmental SEM with EDX attachment for elemental composition analysis. FT-IR spectra were collected with a NICOLET iS5 spectrometer from Thermo Scientific, Inc. Each spectrum was collected in the range 1000–3500 cm^{-1}.

3. Results and discussion

3.1. Characterization of PAN membranes

Fig. 2 shows the SEM images of electrospun PAN and MC-decorated PAN nanofibers.

All three samples showed similar fiber morphology. Less nodules were observed for electrospun PAN membrane (Fig. 2A) and 1.0 wt% MC-embedded PAN membrane by electrospinning (Fig. 2C), while 0.5 wt% MC-soaked PAN membrane (Fig. 2B) appears to be more densely packed with a few nodules presented, possibly resulting from the presence of ethanol in the 0.5 wt% MC solution. The fiber diameters of electrospun PAN were in the range of 336–825 nm [520 ± 132 nm, Fig. 2A], whereas the fiber diameters of 0.5 wt% MC-coated PAN and 1.0 wt% MC-embedded PAN were in the range of 344–925 nm [515 ± 162 nm; Fig. 2B] and 562–1584 nm [1030 ± 354 nm; Fig. 2C], respectively. At a voltage such as 13 or 15 kV, the difference in fiber diameters could be attributed to highly unstable streams dispersed in different directions [52]. The addition of MC could also be responsible for the increase of the average fiber diameter and higher standard deviation.

Fig. 3 shows the FT-IR spectra of electrospun PAN nanofibers before and after the incorporation of MC. In the FT-IR spectrum of PAN nanofibers (Fig. 3d), the absorption peak of 2245 cm^{-1} could be attributed to the stretching vibration of C≡N in PAN polymer. The other two strong peaks in the ranges of 1730–1737 cm^{-1} and 1455–1460 cm^{-1} correspond to the stretching vibration of C═O and the bending vibration of C—H, respectively [53]. In the FTIR spectrum of MC (Fig. 3c), the absorption peaks near 1710 cm^{-1} could be attributed to the stretching vibration of C═O in MC [48]. The distinctive characteristic vibrational

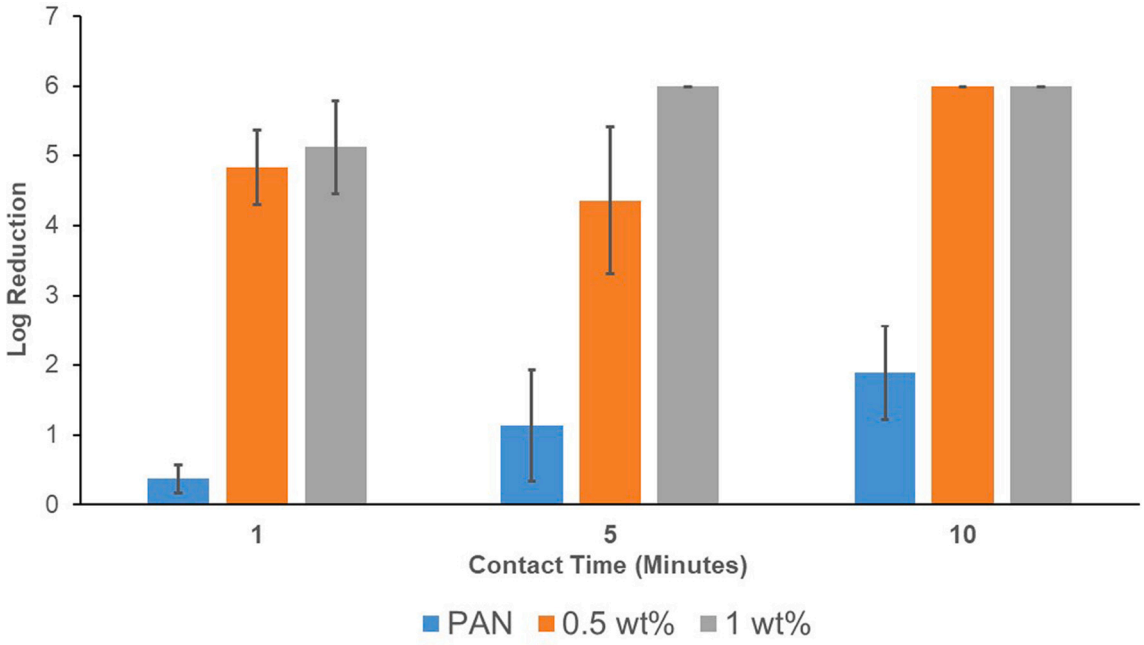

Fig. 4. Antimicrobial efficacy of PAN nanofibers against *Klebsiella pneumoniae* (ATCC 13882). PAN: Control; 0.5 wt%: PAN after soaking in 0.5 wt% MC for 2 min; 1.0 wt%: PAN embedded with 1.0 wt% MC via electrospinning.

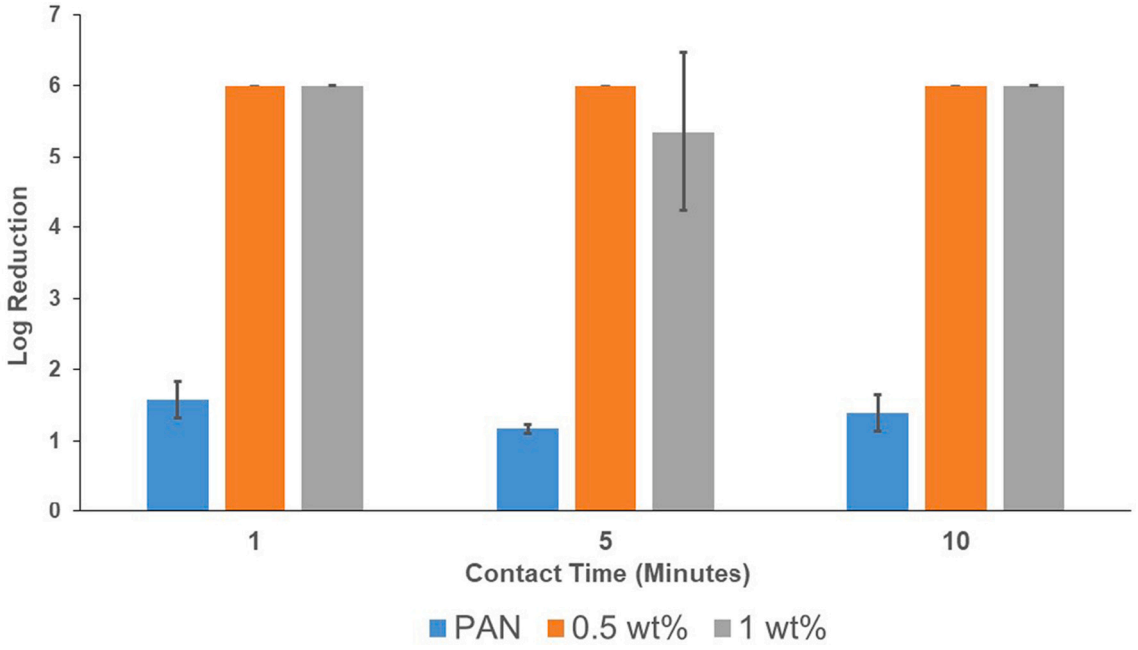

Fig. 5. Antimicrobial efficacy of nanofibers against *E. coli* (K12). PAN: control; 0.5 wt%: PAN after soaking in 0.5 wt% MC for 2 min; 1.0 wt%: PAN embedded with 1.0 wt% MC via electrospinning.

bands of 1706 and 1717 cm^{-1} of MC were detected in both 0.5 wt% MC-soaked PAN (Fig. 3a) and 1.0 wt% MC-embedded PAN (Fig. 3b) membranes, indicating that MC was successfully incorporated into the PAN nanofibers. The enhancement of the peak intensity of 1717 cm^{-1} observed in 0.5 wt% MC-soaked PAN membrane could be explained by the solvent effect on carbonyl stretching frequency by the presence of ethanol [54].

Blend electrospinning is known to be able to encapsulate hydrophilic and lipophilic entities as well as biomolecules (such as RNA, DNA, and proteins) into the fiber [55]. However, the distribution of encapsulated molecules in nanofibers is uneven, with the majority of them being embedded inside the fiber, and a small percentage being exposed to the outer surface of the fiber. In this study, electrospun PAN nanofibers are intrinsically hydrophobic in nature [56]. MC is an organic chemical with one nitrogen-containing ring and four hydrophobic methyl groups, and is slightly soluble in water [57]. The chlorine contents in the MC-treated nanofibers were found to be $0.0029 \pm 4.1 \times 10^{-4}$% and $0.0014 \pm 2.5 \times 10^{-4}$% (*w*/w) for 0.5 wt% MC-soaked PAN and 1.0 wt% MC embedded PAN nanofibers, respectively. The results suggest that surface-coated MC after the soaking process could be more accessible than those embedded inside the PAN polymer membrane during the blend electrospinning process. The encapsulated molecules inside the fiber are mainly released through simple surface diffusion and pores caused by the degradation of the fiber [55], the release profile of poorly water-soluble MC molecules could be enhanced by the creation of carefully-chosen dual polymer systems [58] or core-sheath nanofibers [21].

3.2. Antimicrobial efficacy against liquid bacterial suspensions

The antibacterial test results of PAN nanofibers against *Klebsiella*

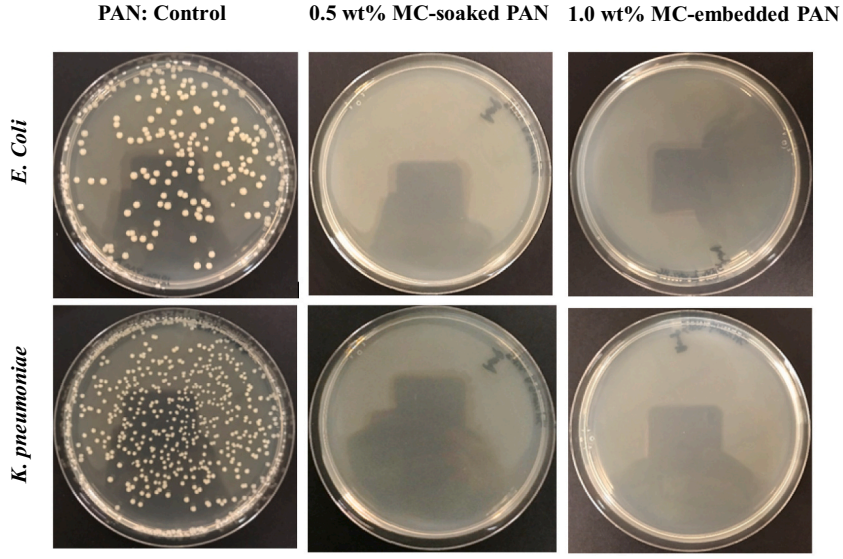

Fig. 6. Representative Petri plate images showing (Top) and (Bottom) *Klebsiella pneumoniae* colonies growth after 10 min of contact.

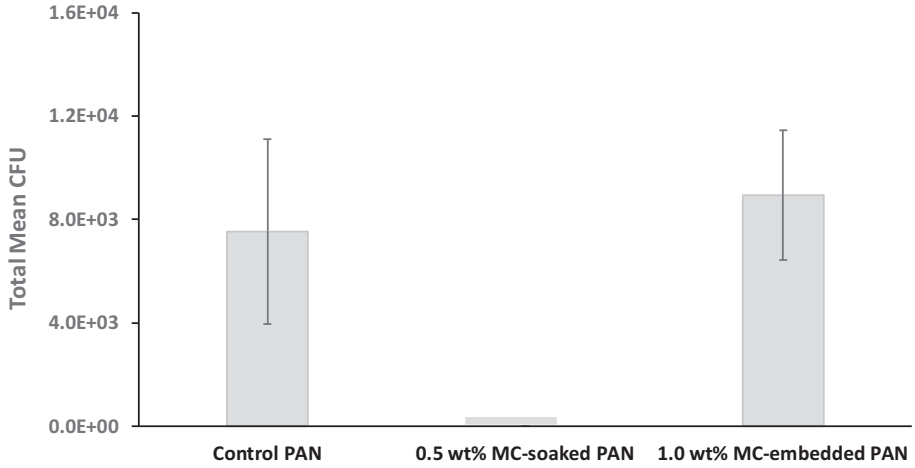

Fig. 7. Antimicrobial efficacy of PAN nanofibers against aerosolized *E. coli* (ATCC15597).

pneumoniae using the sandwich method are shown in Fig. 4. The *K. pneumoniae* bacteria were reduced by 4.8, 4.5, and 6.0 log after a 1, 5, 10 min incubation in 0.5 wt% MC-coated PAN nanofibers, and reduced by 5.0, 6.0 and 6.0 log in 1.0 wt% MC-embedded PAN nanofibers, whereas the bacteria were reduced by 0.2, 1.0, 2.0 log within the same time periods in the blank PAN nanofibers.

Similar changes were also observed for the antibacterial test against *E. coli* (K12) (Fig. 5). The *E. coli* (K12) bacteria were reduced by 6.0, 6.0, and 6.0 log after a 1, 5, 10 min incubation in 0.5 wt% MC-coated PAN nanofibers, and reduced by 6.0, 5.4 and 6.0 log in 1.0 wt% MC-embedded PAN nanofibers, whereas the bacteria were reduced by 1.5, 1.0, 1.2 log within the same time periods in the blank PAN nanofibers.

The results demonstrated that the bacterial reduction in 0.5 wt% MC-coated PAN nanofibers was similar to 1.0 wt% MC-embedded PAN nanofibers, indicating that the current oxidative chlorine content was sufficient for killing bacteria effectively, and the two methods used to incorporate MC into the PAN nanofibers had minimal effect on bacterial death. The variation in the log reduction between the different batches of samples against the same bacteria was most likely due to the weight differences of the coupons. HOCl, a hydrolysis product of MC, is a strong oxidizing agent that can oxidize the sulfhydryl groups of enzymes leading to impaired cellular function, and eventually cell death [59]. The slight difference in the antimicrobial efficacy of MC-decorated PAN membranes against different types of bacteria could be due to the structural variations of different bacterial components. In all cases, the bacterial reduction ratio increased with increasing contact time, demonstrating that the production of HOCl by the hydrolysis of MC is a time-dependent process. Overall, MC-decorated PAN nanofibers successfully inhibited the growth of *K. pneumonia* and *E. coli* (K12) within minutes of contact (as shown in Fig. 6).

3.3. Antimicrobial efficacy against bacterial bioaerosols

The embedding of inactivating components in a face mask filter provides a very attractive way for mitigating the health risks caused by invisible airborne pathogens. To gain insights into the antimicrobial effect of MC-decorated PAN nanofibers on aerosolized bacteria, we investigated their antimicrobial efficacy against aerosolized *E. coli*. The bioaerosol was generated using a 3-jet collision nebulizer and a liquid suspension of *E. coli* (ATCC 15597). Each electrospun membrane (blank PAN, 0.5 wt% MC-soaked PAN, and 1.0 wt% MC-embedded PAN) was loaded with aerosolized *E. coli* for 10 min and subsequently incubated at room temperature for 30 min to allow for sufficient contact with the MC. The *E. coli* was removed from the filters using 0.01 M sodium thiosulfate and plated for viable counts.

As shown in Fig. 7, the total mean amount of viable *E. coli* recovered from the control PAN was 7.53×10^3 CFU. The 1.0 wt% MC-embedded PAN nanofibers did not have any antimicrobial effect on the aerosolized *E. coli* with a total mean recovery of 8.93×10^3 CFU. However, the 0.5 wt% MC-soaked PAN membrane was very effective at inactivating *E. coli* since no viable counts were obtained. The minimal antibacterial effect observed by the MC-embedded PAN nanofibers on aerosolized *E. coli* is likely due to a negligible amount of oxidative chlorine produced on the surface of the PAN nanofibers within the limited time of exposure. In the current study, the bioaerosol inactivation experiment involved a 10-min loading step and a 30-min incubation step. Although the aerosol collected onto the PAN nanofibers was a wet aerosol, the 10-min loading time likely allowed for impaction to occur primarily on the outer surface of the electrospun material and not deep within the inner surfaces. This would hinder the release of MC molecules from the inner surface to the outer surface including the production of HOCl by the hydrolysis of MC. This was not the case for microorganisms in liquid suspension which showed equivalent log reduction of viability when exposed to MC-soaked PAN versus MC-embedded PAN. The liquid state allowed for a quick release of the inner surface MC and the production of HOCl hydrolysis for the MC-embedded PAN. Furthermore, the amount of accessible MC molecules on the surface of MC-embedded electrospun PAN nanofiber was much less than those on the surface of MC-soaked electrospun PAN nanofibers, which was reflected by the presence of higher chlorine content in the latter sample, as determined by the iodometric/thiosulfate titration.

The MC-soaked PAN membrane was able to inactivate 99.9% of the aerosolized *E. coli* within 30 min of contact. The antimicrobial efficacy of 0.5 wt% MC-soaked PAN membrane was superior than that reported by others, in which a 6.0 log reduction was observed after *S. aureus* bioaerosol was exposed to a 5.0 wt% MC-embedded PAN membrane [48] or 1.0 wt% MC-coated polypropylene nonwoven fabric [39] for 3 h. The results suggest the amount of MC on the surface of 0.5 wt%-soaked PAN membranes was much higher than that of 1.0 wt% or 5.0 wt% MC-embedded PAN membranes.

4. Conclusions

In summary, we report the first comparative study of the efficacy of MC-functionalized electrospun PAN nanofibers prepared by blend electrospinning and soaking, on the inactivation of bacteria in both liquid and aerosol forms. Functional antimicrobial electrospun PAN nanofibers were prepared using MC as the disinfectant agent. The MC-decorated PAN membranes were successfully fabricated by using a one-step blend electrospinning process with a mixture solution of 1.0 wt % MC and 8 wt% PAN in DMF and by soaking electrospun PAN membranes in 0.5 wt% MC in ethanol for 2 min. The surface morphology of

MC-decorated PAN membranes changed slightly from the blank PAN membrane, however the porous structure remained intact after the soaking by 0.5 wt% MC in ethanol, or blend electrospinning in the presence of 1.0 wt% MC. The antimicrobial efficacy testing with 0.5 wt% MC-soaked PAN and 1.0 wt% MC-embedded PAN nanofibers demonstrated that MC-decorated PAN nanofibers successfully inhibited the growth of *Klebsiella pneumoniae* and *E. coli* in less than 1 min. In addition, 0.5 wt% MC-soaked PAN showed excellent disinfection efficacy against aerosolized *E. coli* in 30 min. Between these two methods, the blend electrospinning method is less labor-intensive and offers higher loading efficiency, however, its release kinetics of the poorly water-soluble MC from the hydrophobic electrospun PAN nanofibers remain to be optimized for inactivation of bioaerosols. The soaking method uses much less amount of MC and is more cost-effective, thus making it more suitable for large-scale production. The simplicity, cost-effectiveness, versatility, and scalability of the electrospinning process, together with the superior antimicrobial activity of N-halamines make it a promising solution for improving drinking water quality and for mitigating respiratory pathogen transmission.

Author contributions

F. Y., L. H., and J. K. designed the experiments. M. G.C. performed the majority of the experiments, together with B. C. for electrospinning, and N.W. for antibacterial assays. L. H. performed SEM and data analysis. J. K. performed bioaerosol studies and data analysis. All authors reviewed and revised the manuscript.

Data availability

The raw/processed data required to reproduce these findings cannot be shared at this time as the data also forms part of an ongoing study.

Declaration of Competing Interest

The authors declare that they have no known competing financial interests or personal relationships that could have appeared to influence the work reported in this paper.

Acknowledgments

M. G. C., B. C. and F. Y., are grateful for the financial support of this project by the U.S. National Science Foundation (Awards # 1831133 and #2122044). The authors thank Dr. Yanan Zhang and Dr. Dehui Zhang for their assistance in synthesis and characterization of MC and Dr. Howard Walls for his help in optimizing the loading of aerosolized *E. coli*.

References

[1] P.K. Pandey, P.H. Kass, M.L. Soupir, S. Biswas, V.P. Singh, Contamination of water resources by pathogenic bacteria, AMB Express 4 (2014) 51, https://doi.org/10.1186/s13568-014-0051-x.

[2] K. Kim, E. Kabir, S. Ara Jahan, Airborne bioaerosols and their impact on human health, J. Environ. Sci. 67 (2018) 23–35, https://doi.org/10.1016/j.jes.2017.08.027.

[3] WHO Factsheets on Drinking Water. https://www.who.int/news-room/fact-sheets/detail/drinking-water, 2019 (accessed 7 June 2021).

[4] WHO Coronavirus (COVID-19) Dashboard. https://covid19.who.int/, 2021 (accessed on 8 June 2021).

[5] A. Chaudhary, A. Gupta, R.B. Mathur, S.R. Dhakate, Effective antimicrobial filter from electrospun polyacrylonitrile-silver composite nanofibers membrane for conducive environment, Adv. Mater. Lett. 5 (2014) 562–568, https://doi.org/10.5185/amlett.2014.572.

[6] I. Buchovec, V. Lukseviciūtė, R. Kokstaite, D. Labeikyte, L. Kaziukonyte, Z. Luksiene, Inactivation of Gram (−) bacteria *Salmonella enterica* by chlorophyllin-based photosensitization: mechanism of action and new strategies to enhance the inactivation efficiency, J. Photochem. Photobiol. B 172 (2017) 1–10, https://doi.org/10.1016/j.jphotobiol.2017.05.008.

[7] P. Li, L. Li, Y. Wang, T. Zheng, J. Liu, Characterization, factors, and UV reduction of airborne bacteria in a rural wastewater treatment station, Sci. Total Environ. 751 (2021) 141811, https://doi.org/10.1016/j.scitotenv.2020.141811.

[8] J. You, Y. Guo, R. Guo, X. Liu, A review of visible light-active photocatalysts for water disinfection: features and prospects, Chem. Eng. J. 373 (2019) 624–641, https://doi.org/10.1016/j.cej.2019.05.071.

[9] G.U. Afewerki, A. Ruiz-Esparza, O. Lobo, Antimicrobial electrospun materials, in: I. R. Boddula, M.I. Ahamed, A.M. Asiri (Eds.), Electrospun Materials and Their Allied Applications, Scrivener Publishing LLC, 2020, pp. 243–264.

[10] M. Rahmati, D.K. Mills, A.M. Urbanska, M.R. Saeb, J.R. Venugopal, S. Ramakrishna, M. Mozafari, Electrospinning for tissue engineering applications, Prog. Mater. Sci. 117 (2021) 100721, https://doi.org/10.1016/j.pmatsci.2020.100721.

[11] Y. Lu, X. Xiao, J. Fu, C. Huan, S. Qi, Y. Zhan, Y. Zhu, G. Xu, Novel smart textile with phase change materials encapsulated core-sheath structure fabricated by coaxial electrospinning, Chem. Eng. J. 355 (2019) 532–539, https://doi.org/10.1016/j.cej.2018.08.189.

[12] J. Cui, T. Lu, F. Li, Y. Wang, J. Lei, W. Ma, Y. Zou, C. Huang, Flexible and transparent composite nanofibre membrane that was fabricated via a "green" electrospinning method for efficient particulate matter 2.5 capture, J. Colloid Interface Sci. 582 (2021) 506–514, https://doi.org/10.1016/j.jcis.2020.08.075.

[13] I. Tlili, T.A. Alkanhal, Nanotechnology for water purification: electrospun nanofibrous membrane in water and wastewater treatment, J. Water Reuse Desal. 9 (2019) 232–248, https://doi.org/10.2166/wrd.2019.057.

[14] Z. Li, Z. Ma, X. Zhang, Q. Du, Y. Fu, L. Shuang, K. Yang, L. Li, W. Lai, W. Zhang, In-situ growth NiMoS3 nanoparticles onto electrospinning synthesis carbon nanofibers as a low cost platinum-free counter electrode for dye-sensitized solar cells, J. Alloys Compd. 850 (2021) 156807, https://doi.org/10.1016/j.jallcom.2020.156807.

[15] X. Zhao, D. Wang, S. Liu, Z. Li, J. Meng, Y. Ran, Y. Zhang, L. Li, Bi2S3 nanoparticles densely grown on electrospun-carbon-nanofibers as low-cost counter electrode for liquid-state solar cells, Mater. Res. Bull. 125 (2020) 110800, https://doi.org/10.1016/j.materresbull.2020.110800.

[16] K. Ghosal, R. Augustine, A. Zaszczynska, M. Barman, A. Jain, A. Hasan, N. Kalarikkal, P. Sajkiewicz, S. Thomas, Novel drug delivery systems based on triaxial electrospinning based nanofibers, React. Funct. Polym. 163 (2021) 104895, https://doi.org/10.1016/j.reactfunctpolym.2021.104895.

[17] A. Luraghi, F. Peri, L. Moroni, Electrospinning for drug delivery applications: A review, J. Control. Release 334 (2021) 463–484, https://doi.org/10.1016/j.jconrel.2021.03.033.

[18] C. Chen, Y. Tang, B. Vlahovic, F. Yan, Electrospun polymer nanofibers decorated with noble metal nanoparticles for chemical sensing, Nanoscale Res. Lett. 12 (2017) 451, https://doi.org/10.1186/s11671-017-2216-4.

[19] A. Oner, E. Tufek, I. Yezer, A. Birol, M. Demir, S. Er, D.O. Demirkol, High generation dendrimer decorated poly-Ɛ-caprolactone/polyacrylic acid electrospun nanofibers for the design of a bioelectrochemical sensing surface, React. Funct. Polym. 161 (2021) 104853, https://doi.org/10.1016/j.reactfunctpolym.2021.104853.

[20] S. Kang, S. Hou, X. Chen, D.-G. Yu, L. Wang, X. Li, G. Williams, Energy-saving electrospinning with a concentric Teflon-core rod spinneret to create medicated nanofibers, Polymers 12 (2020) 2421, https://doi.org/10.3390/polym12102421.

[21] H. Xu, X. Xu, S. Li, W. Song, D.-G. Yu, S.W. Annie Bligh, The effect of drug heterogeneous distributions within core-sheath nanostructures on its sustained release profiles, Biomolecules 11 (2021) 1330, https://doi.org/10.3390/biom11091330.

[22] M. Wang, J. Hou, D.-G. Yu, S. Li, J. Zhu, Z. Chen, Electrospun tri-layer nanodepots for sustained release of acyclovir, J. Alloys Compd. 846 (2020) 156471, https://doi.org/10.1016/j.jallcom.2020.156471.

[23] M. Wang, D. Li, J. Li, S. Li, Z. Chen, D.-G. Yu, Z. Liu, J.Z. Guo, Electrospun Janus zein–PVP nanofibers provide a two-stage controlled release of poorly water-soluble drugs, Mater. Des. 196 (2020) 109075, https://doi.org/10.1016/j.matdes.2020.109075.

[24] D. Li, M. Wang, D.-G. Yu Song, S.W. Annie Bligh, Electrospun Janus beads-on-a-string structures for different types of controlled release profiles of double drugs, Biomolecules 11 (2021) 635, https://doi.org/10.3390/biom11050635.

[25] S. Chen, R. Li, X. Li, J. Xie, Electrospinning: an enabling nanotechnology platform for drug delivery and regenerative medicine, Adv. Drug Deliv. Rev. 132 (2018) 188–213, https://doi.org/10.1016/j.addr.2018.05.001.

[26] N.G. Rim, C.S. Shin, H. Shin, Current approaches to electrospun nanofibers for tissue engineering, Biomed. Mater. 8 (2013), 014102.

[27] Y.J. Son, W.J. Kim, H.S. Yoo, Therapeutic applications of electrospun nanofibers for drug delivery systems, Arch. Pharm. Res. 37 (2014) 69–78, https://doi.org/10.1007/s12272-013-0284-2.

[28] X. Qin, S. Subianto, Chapter 17 - Electrospun nanofibers for filtration applications, in: Mehdi Afshari (Ed.), Woodhead Publishing Series in Textiles, Electrospun Nanofibers, Woodhead Publishing, 2017, pp. 449–466.

[29] M. Gorji, R. Bagherzadeh, H. Fashandi, Chapter 21 - Electrospun nanofibers in protective clothing, in: Mehdi Afshari (Ed.), Woodhead Publishing Series in Textiles, Electrospun Nanofibers, Woodhead Publishing, 2017, pp. 571–598.

[30] M. Liu, X. Duan, Y. Li, D. Yang, Y. Long, Electrospun nanofibers for wound healing, Mater. Sci. Eng. C 76 (2017) 1413–1423, https://doi.org/10.1016/j.msec.2017.03.034.

[31] A. Chinnappan, C. Baskar, S. Baskar, G. Ratheesh, S. Ramakrishna, An overview of electrospun nanofibers and their application in energy storage, sensors and wearable/flexible electronics, J. Mater. Chem. C 5 (2017) 12657–12673, https://doi.org/10.1039/C7TC03058D.

[32] J. Quirós, J.P. Borges, K. Boltes, I. Rodea-Palomares, R. Rosal, Antimicrobial electrospun silver-, copper- and zinc-doped polyvinylpyrrolidone nanofibers, J. Hazad. Mater. 299 (2015) 298–305, https://doi.org/10.1016/j.jhazmat.2015.06.028.
[33] H. Rodríguez-Tobías, G. Morales, A. Ledezma, J. Romero, D. Grande, Novel antibacterial electrospun mats based on poly (D, L-lactide) nanofibers and zinc oxide nanoparticles, J. Mater. Sci. 49 (2014) 8373–8385, https://doi.org/10.1007/s10853-014-8547-y.
[34] L. Chang, J. Wang, C. Tong, L. Zhao, X. Liu, Comparison of antimicrobial activities of polyacrylonitrile fibers modified with quaternary phosphonium salts having different alkyl chain lengths, J. Appl. Polym. Sci. 133 (2016) 43689, https://doi.org/10.1002/app.43689.
[35] E. Gliścińska, B. Gutarowska, B. Brycki, I. Krucińska, Electrospun polyacrylonitrile nanofibers E. modified by quaternary ammonium salts, J. Appl. Polym. Sci. 128 (2013) 767–775, https://doi.org/10.1002/app.38210.
[36] A. Dong, Y. Wang, Y. Gao, T. Gao, G. Gao, Chemical insights into antibacterial N-Halamines, Chem. Rev. 117 (2017) 4806–4862, https://doi.org/10.1021/acs.chemrev.6b00687.
[37] F. Hui, C. Debiemme-Chouvy, Antimicrobial N-halamine polymers and coatings: a review of their synthesis, characterization, and applications, Biomacromolecules 14 (2013) 585–601, https://doi.org/10.1021/bm301980q.
[38] G. Sun, T.Y. Chen, M.S. Habercom, W.B. Wheatley, S.D. Worley, Performance of a new polymeric water disinfectant, J. Am. Water Res. Assoc. 32 (1996) 793, https://doi.org/10.1111/j.1752-1688.1996.tb03476.
[39] B. Demir, I. Cerkez, S.D. Worley, R.M. Broughton, T.S. Huang, N-halamine-modified antimicrobial polypropylene nonwoven fabrics for use against airborne bacteria, ACS Appl. Mater. Interfaces 7 (2015) 1752–1757, https://doi.org/10.1021/am507329m.
[40] X. Sun, Z. Cao, N. Porteous, Y. Sun, An N-halamine-based rechargeable antimicrobial and biofilm controlling polyurethane, Acta Biomater. 8 (2012) 1498–1506, https://doi.org/10.1016/j.actbio.2011.12.027.
[41] T. Ren, T.V. Dormitorio, M. Qiao, T. Huang, J. Weese, N-halamine incorporated antimicrobial nonwoven fabrics for use against avian influenza virus, Vet. Microbiol. 218 (2018) 78–83, https://doi.org/10.1016/j.vetmic.2018.03.032.
[42] G. Sun, X. Xu, Durable and regenerable antibacterial finishing of fabrics. Antimicrobial properties, Text. Chem. Color. 30 (1998) 26–30.
[43] G. Sun, S.D. Worley, Chapter 6 Halamine chemistry and its application in antimicrobial textiles and polymers, in: Edwards (Ed.), Modified Fibers with Medical and Specialty Applications, 2006, pp. 81–89.
[44] H. Tian, Y. Zhai, C. Xu, J. Liang, Durable antibacterial cotton fabrics containing stable acyclic N-Halamine groups, Ind. Eng. Chem. Res. 56 (2017) 7902–7909, https://doi.org/10.1021/acs.iecr.7b00863.
[45] https://drjohnson.com/whats-in-tetras-lifeguard-product-and-what-does-it-do/ (accessed on 8 June 2021).
[46] M.S.A. Rahaman, A.F. Ismail, A. Mustafa, A review of heat treatment on polyacrylonitrile fiber, Polym. Degrad. Stab. 92 (2007) 1421–1432, https://doi.org/10.1016/j. polymdegradstab. 2007.03.023.
[47] L. Zhang, J. Luo, T.J. Menkhaus, H. Varadaraju, Y. Sun, H. Fong, Antimicrobial nano-fibrous membranes developed from electrospun polyacrylonitrile nanofibers, J. Membr. Sci. 369 (2011) 499–505, https://doi.org/10.1016/j.memsci.2010.12.032.
[48] C. Huang, Y. Liu, Z. Li, R. Li, X. Ren, T.S. Huang, N-halamine antibacterial nanofibrous mats based on polyacrylonitrile and N-halamine for protective face masks, J. Eng. Fib. Fabrics 14 (2019) 1–8, https://doi.org/10.1177/1558925019843222.
[49] X. Ren, L. Kou, H.B. Kocer, C. Zhu, S.D. Worley, R.M. Broughton, T. Huang, Antimicrobial coating of an N-halamine antimicrobial monomer on cotton fibers via admicellar polymerization, Colloid. Surf. A 317 (2008) 711–716, https://doi.org/10.1016/j.colsurfa.2007.12.007.
[50] 48] W. Li, X. Xie, Q. Shi, H. Zeng, Y. Ouyang, Y. Chen, Antibacterial activity and mechanism of silver nanoparticles on *Escherichia coli*, Appl. Microbiol. Biotechnol. 85 (2010) 1115–1122, https://doi.org/10.1007/s00253-009-2159-5.
[51] ASTM F2101 - 01, Standard Test Method for Evaluating the Bacterial Filtration Efficiency (BFE) of Medical Face Mask Materials, Using a Biological Aerosol of *Staphylococcus aureus*. https://www.astm.org/DATABASE.CART/HISTORICAL/F2101-01.htm.
[52] X. Ren, H.B. Kocer, S.D. Worley, R.M. Broughton, T.S. Huang, Biocidal nanofibers via electrospinning, J. Appl. Polym. Sci. 127 (2013) 3192–3197, https://doi.org/10.1002/app.37731.
[53] S. Li, Y. Wang, L. Ma, X. Zhang, S. Dong, L. Liu, X. Zhou, C. Wang, Z. Shi, Synthesis of PAN with adjustable molecular weight and low polydispersity index (PDI) value via reverse atom transfer radical polymerization, Design. Monom. Polym. 22 (2019) 180–186, https://doi.org/10.1080/15685551.2019.1678557.
[54] C. Parlak, P. Ramasami, Theoretical and experimental study of infrared spectral data of 2-bromo-4-chlorobenzaldehyde, SN Appl. Sci. 2 (2020) 1148, https://doi.org/10.1007/s42452-020-2935-5.
[55] Y. Sun, S. Cheng, W. Lu, Y. Wang, P. Zhang, Q. Yao, Electrospun fibers and their application in drug controlled release, biological dressings, tissue repair, and enzyme immobilization, RSC Adv. 9 (2019) 25712–25729, https://doi.org/10.1039/C9RA05012D.
[56] M.N. Sarwar, A. Ullah, M.K. Haider, N. Hussain, S. Ullah, M. Hashmi, M.Q. Khan, I. S. Kim, Evaluating antibacterial efficacy and bocompatibility of PAN nanofibers loaded with diclofenac sodium salt, Polymers 13 (2021) 510, https://doi.org/10.3390/polym13040510.
[57] Y. Zheng, N. Pan, Y. Liu, X. Ren, Novel porous chitosan/N-halamine structure with efficient antibacterial and hemostatic properties, Carbohydr. Polym. 253 (2021) 117205, https://doi.org/10.1016/j.carbpol.2020.117205.
[58] J.D. Orlando, T.B. Limbu, B. Chitara, F. Yan, One-pot electrospinning of polyvinylpyrrolidone/cellulose acetate/TiO2 nanofibrous membranes with enhanced photocatalytic properties, J. Porous. Mater. 27 (2020) 911–918, https://doi.org/10.1007/s10934-020-00866-4.
[59] S. Bloomfield, E. Uso, The antibacterial properties of sodium hypochlorite and sodium dichloroisocyanurate as hospital disinfectants, J. Hosp. Infect. 6 (1985) 20–30, https://doi.org/10.1016/s0195-6701(85)80014-1.